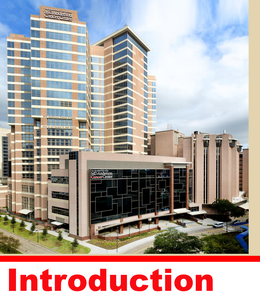

Pre-clinical efficacy of CDK7 inhibitor-based combinations in cellular models of advanced myeloproliferative neoplasms (MPN) transformed to AML

Warren Fiskus[1], Prithviraj Bose[1], Lucia Masarova[1], Christopher P. Mill[1], Christine E. Birdwell[1], John A. Davis[1], Kaberi Das[1], Hanxi Hou[1], Taghi Manshouri[1], Kevin Philip[1], Noor Alhamadani[1], Alicia Matthews[1], Sanam Loghavi[1] and Kapil N. Bhalla[1]

[1]The University of Texas MD Anderson Cancer Center, Houston, TX

THE UNIVERSITY OF TEXAS MD Anderson Cancer Center

Making Cancer History®

Poster Session Online

American Society of Hematology — Helping hematologists conquer blood diseases worldwide

631. Myeloproliferative Syndromes and Chronic Myeloid Leukemia: Basic and Translational: Poster I

Warren Fiskus

SAT-1783

ASH2023

Introduction

Stem/progenitor cells in advanced-MPN express pathogenetic, disease-defining, driver mutations in JAK2, c-MPL or calreticulin (CALR) gene, and display constitutive activation of JAK-STAT5/3 and NFkB signaling, which is responsible for the aberrant biology, phenotype and clinical features of MPN. These include 2+ myelofibrosis, extramedullary hematopoiesis, splenomegaly, and inflammatory cytokine-driven constitutional symptoms. Treatment with type I JAK1/2 inhibitor (JAKi), including ruxolitinib, confers notable clinical benefit by reducing spleen size, constitutional symptoms, and modest improvement in patient survival. Clinical utility of JAKi in advanced MPN is undermined by adverse side effects, persistent JAK2/STAT3/5 signaling despite JAKi treatment, and due to progression to MPN-BP. Accumulation of additional mutations in chromatin/transcriptional regulators (epimutations) in MPN stem/progenitor cells, including DNMT3A, TET2, ASXL1, EZH2, SRSF2, RUNX1 and TP53, lead to progression to MPN-EB (> 5% blasts in BMA or PB) including accelerated phase (AP) (10-19% blasts) or sAML (20% or more blasts). JAKi treatment fails to check progression of the disease. JAKi such as ruxolitinib alone or in combination with standard AML therapy, including hypomethylating agents and venetoclax, also do not significantly alter the clinical outcome in MPN-EB/AP/sAML, where the median survival is less than 6 months. Collectively, these observations underscore an unmet need to develop and test rationally targeted, novel agents and combination therapies for advanced-MPN with EB/AP/sAML. In advanced MPN stem/progenitor cells, co-occurrence of the driver mutations and co-mutations creates the dysregulated transcriptome and proteome, which is responsible for the increased growth, cell-survival and therapy-refractoriness. The dysregulated transcriptome is created by binding of TFs to enhancers and promoters, followed by mRNA transcript initiation and elongation. This is dependent on mediator bound PIC (pre-initiation complex) containing the general transcript initiation factors e.g., TFIIH, recruitment of HATs (histone acetyltransferases), the BET protein BRD4 and pTEFb (a heterodimer composed of CDK9 and cyclin T), as well as on the activity of RNA pol II (RNAP2). CDK7 bound to its regulatory cyclin H is the crucial catalytic component of TFIIH (also containing MAT1), which is recruited to transcription start-sites along with RNAP2 to initiate transcription. CDK7 phosphorylates serine 5 and 7 in the C-terminal domain (CTD) of RNAP2, facilitating mRNA transcript initiation. CDK7 also phosphorylates CDK9 (in pTEFb), which in turn phosphorylates serine 2 of the CTD of RNAP2, and phosphorylates and inactivates the negative elongation factors, thus enabling productive transcription of oncogenes. These include MYC, Bcl-xL, CDK4/6, PIM1 and RUNX1, as well as MCL1, which are critical for promoting cell growth and survival of MPN-EB/AP/sAML cells. In a separate role, complexed with cyclin H and MAT1, CDK7 also phosphorylates cell-cycle regulatory CDK1, 2, 4 and 6. Thus, targeted inhibition of CDK7 could potentially abrogate the dysregulated transcriptome and inhibit growth and survival of advanced-MPN and MPN-EB/AP/sAML cells. Indeed, the CRISPR-gRNA dependency-screen (DepMap) demonstrated that CDK7 is a dependency in the advanced-MPN cell lines, SET2 and HEL92.1.7 (HEL). Additionally, higher CDK7 expression was noted in post-MPN sAML samples in the BEAT AML data set. Recently, potent, selective, covalent and ATP-competitive, CDK7 inhibitors (CDK7i), such as SY-1365, and its clinical grade counterpart SY-5609 (Syros Pharmaceuticals), have been developed. In the present studies, we demonstrate that treatment with SY-1365 and SY-5609, dose-dependently affect cell cycle progression and induced in vitro loss of viability in HEL and SET2 cells, as well as in patient-derived (PD), CD34+ MPN-sAML but not in normal CD34+ progenitor cells. We also determined that CDK7 depletion significantly reduced SY-5609-mediated loss of viability. Importantly, pre-treatment with SY-5609 significantly increased sensitivity to ruxolitinib-induced loss of viability in JAKi-resistant SET2 and HEL cells, suggesting that CDK7 inhibition could overcome resistance to JAKi in MPN-sAML cells. We also demonstrate by RNA-Seq analysis that SY5609 negatively-enriched gene sets including MYC and E2F targets with significant decline in MYC, MYB, PLK1/4, KIT, CDK6, AURKA, PIM1 and CCND1, but upregulation of CDKN1A and HEXIM1. We also performed mass spectrometry analysis following SY-5609 treatment which demonstrated significant decline in c-Myc, c-Myb, RUNX1, PLK1, PIM1, but increase in p21, CASP9, BAD, DAP and TGFB1 protein levels. CyTOF analysis demonstrated that SY-5609 treatment markedly reduced c-Myc, RUNX1 and MCL1, while increasing TP53, p21, and cleaved PARP proteins levels in phenotypically defiend MPN-sAML stem-progenitor cells. We next determined that co-treatment with SY-5609 and ruxolitinib induced synergistic loss of viability in HEL, SET2 and PD MPN-sAML cells (n = 5) (delta synergy scores > 1.0 by the ZIP method). A CRISPR screen targeting epigenetic regulators conducted in SET2 and HEL cells revealed significant log2 fold-decline in gRNA targeting BRD4, CBP and p300, highlighting them as dependencies. Consistent with this, co-treatment with SY-5609 and the pan BETi OTX015 or pelabresib or the BD2-selective BETi ABBV-744 or the CBP/p300 inhibitor GNE-049 was synergistically lethal in SET2, HEL, mouse MPN (JAK2-V617F plus TP53 loss) cells and PD MPN-sAML cells (n=5). In the xenograft model of HEL-Luc/GFP cells in NSG mice, monotherapy with SY-5609 vs vehicle control, significantly reduced the MPN-sAML burden and improved survival, without causing toxicity. Additionally, compared to each drug or vehicle control, co-treatment with SY-5609 and OTX015 reduced more MPN-sAML burden and significantly improved survival in a HEL-Luc/GFP xenograft model without inducing toxicity. These findings demonstrate promising preclinical activity of CDK7i against the cellular models of MPN-sAML, and support the rationale to further evaluate in vivo efficacy of CDK7i-based combinations against advanced MPN or MPN-sAML.

Results

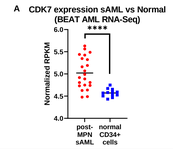

Figure 1. CDK7 expression is higher in post-MPN sAML cells than normal CD34+ cells and is a dependency in sAML HEL92.1.7 and SET2 cells. A. Normalized mRNA expression (RPKM) in post–MPN sAML cells and normal CD34+ cells from the BEAT AML dataset. **** = p < 0.001 for post MPN sAML cells compared to normal CD34+ cells. **B**. CRISPR dependency screen from DepMap. The gene effect shows that CDK7 is a dependency in sAML cell lines HEL92.1.7 and SET2.

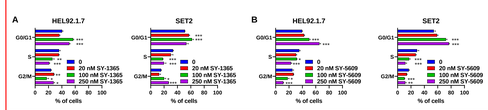

Figure 2. Treatment with CDK7 inhibitor dose dependently induced G1 accumulation and reduced the % of post-MPN sAML cells in S-phase. A-B. HEL92.1.7 and SET2 cells were treated with the indicated concentrations of SY1365 or SY-5609 for 24 hours. Following this, cells were fixed with 70% ethanol; then washed with 1X PBS and stained with propidium iodide. The cell cycle status was determined by flow cytometry. *= p<0.05; **= p< 0.01; *** = p< 0.005 compared to untreated control cells (determined by a two-tailed, unpaired t-test in GraphPad V9).

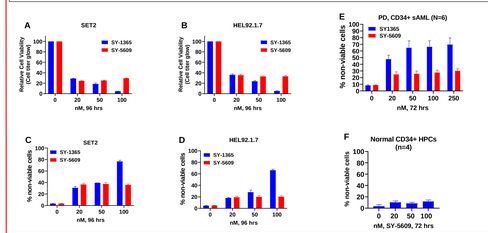

Figure 3. Treatment with CDK7 inhibitor induced loss of viability in cultured and patient-derived CD34+ sAML cells but not normal CD34+ progenitor cells. A-B. SET2 and HEL91.1.7 cells were treated with the indicated concentrations of SY-1365 or SY5609 for 96 hours. At the end of treatment, relative cell viability was determined utilizing a CellTiter-Glo® assay. The % viable cells in each condition was normalized relative to the untreated control cells. Columns, mean of two independent experiments performed in duplicate; Bars, S.E.M. **C-D.** SET2 and HEL91.1.7 cells were treated with the indicated concentrations of SY-1365 or SY5609 for 96 hours. Following this, the cells were washed with 1X PBS and stained with TO-PRO-3 iodide. The % of TO-PRO-3 iodide-positive, non-viable cells was determined by flow cytometry. Columns, mean of three experiments, Bars, S.E.M. **E**. Patient-derived, CD34+ sAML cells were treated with the indicated concentrations of SY-1365 or SY-5609 for 72 hours. Then, the cells were washed with 1X PBS and stained with TO-PRO-3 iodide. The % of TO-PRO-3 iodide-positive, non-viable cells was determined by flow cytometry. Columns, mean of six samples; Bars, S.E.M. **F**. Normal CD34+ HPCs (from umbilical cord blood) were treated with the indicated concentrations of SY-5609 for 72 hours. At the end of treatment, the cells were washed with 1X PBS and stained with TO-PRO-3 iodide. The % of TO-PRO-3 iodide-positive, non-viable cells was determined by flow cytometry. Columns, mean of four samples; Bars, S.E.M.

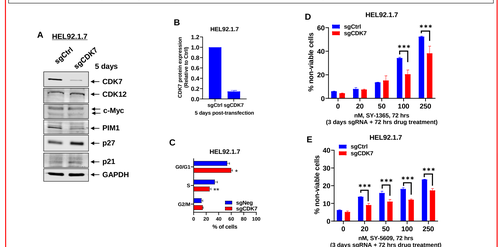

Figure 4. Knockout of CDK7 in sAML HEL92.1.7 cells increases cells in G0/G1 phase while decreasing S-Phase and significantly attenuates the response to CDK7 inhibitors SY-1365 and SY-5609. A. Immunoblot of HEL92.1.7 cells transfected with sgCtrl or sgCDK7 for 5 days. **B**. Quantification of CDK7 knockout. **C**. Cell cycle status of sgCtrl and sgCDK7 transfected cells 5 days post-transfection. **D-E**. HEL cells with sgCtrl or sgCDK7 were treated with SY1365 or SY5609 for 72 hours. The % non-viable cells were determined by flow cytometry. *** = p< 0.005.

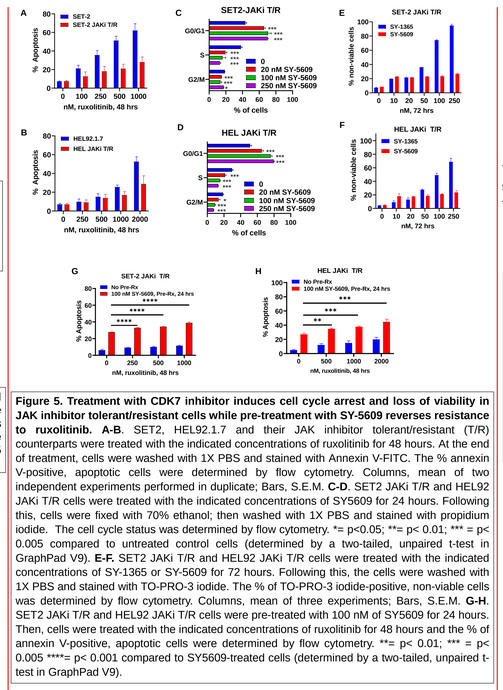

Figure 5. Treatment with CDK7 inhibitor induces cell cycle arrest and loss of viability in JAK inhibitor tolerant/resistant cells while pre-treatment with SY-5609 reverses resistance to ruxolitinib. A-B. SET2, HEL92.1.7 and their JAK inhibitor tolerant/resistant (T/R) counterparts were treated with the indicated concentrations of ruxolitinib for 48 hours. At the end of treatment, cells were washed with 1X PBS and stained with Annexin V-FITC. The % annexin V-positive, apoptotic cells were determined by flow cytometry. Columns, mean of two independent experiments performed in duplicate; Bars, S.E.M. **C-D**. SET2 JAKi T/R and HEL92 JAKi T/R cells were treated with the indicated concentrations of SY5609 for 24 hours. Following this, cells were fixed with 70% ethanol; then washed with 1X PBS and stained with propidium iodide. The cell cycle status was determined by flow cytometry. *= p<0.05; **= p< 0.01; *** = p< 0.005 compared to untreated control cells (determined by a two-tailed, unpaired t-test in GraphPad V9). **E-F.** SET2 JAKi T/R and HEL92 JAKi T/R cells were treated with the indicated concentrations of SY-1365 or SY-5609 for 72 hours. Following this, the cells were washed with 1X PBS and stained with TO-PRO-3 iodide. The % of TO-PRO-3 iodide-positive, non-viable cells was determined by flow cytometry. Columns, mean of three experiments; Bars, S.E.M. **G-H.** SET2 JAKi T/R and HEL92 JAKi T/R cells were pre-treated with 100 nM of SY5609 for 24 hours. Then, cells were treated with the indicated concentrations of ruxolitinib for 48 hours and the % of annexin V-positive, apoptotic cells were determined by flow cytometry. **= p< 0.01; *** = p< 0.005 ****= p< 0.001 compared to SY5609-treated cells (determined by a two-tailed, unpaired t-test in GraphPad V9).

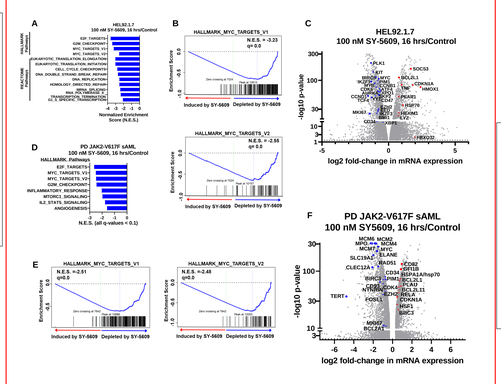

Figure 6. Treatment with SY-5609 causes negative enrichment of MYC targets, E2F targets, cell cycle checkpoints and protein translation initiation and elongation in sAML cells. A. HEL92.1.7 cells (biologic replicates) were treated with 100 nM of SY-5609 for 16 hours. Total RNA was isolated and utilized for RNA-Seq analysis. Gene set enrichment analysis of SY-5609 treated cells compared to HALLMARK and REACTOME pathway datasets. All q-values are < 0.1. **B**. Enrichment plot of SY-5609-treated HEL92.1.7 cells compared to HALLMARK_MYC_TARGETS_V1 and V2 datasets. **C**. Volcano plot of significantly altered mRNAs (p<0.05) in SY-5609-treated HEL92.1.7 cells compared to untreated control cells. **D.** Patient-derived JAK2 V617F-expressing sAML cells (biologic replicates) were treated with 100 nM of SY-5609 for 16 hours. Total RNA was isolated and utilized for RNA-Seq analysis. Gene set enrichment analysis of SY-5609-treated cells compared to HALLMARK and REACTOME pathway datasets. All q-values are < 0.1. **E**. Enrichment plot of SY-5609-treated PD, sAML cells compared to HALLMARK_MYC_TARGETS_V1 and V2 datasets. **F**. Volcano plot of significantly altered mRNAs (p<0.05) in SY-5609-treated PD sAML cells compared to untreated control cells.

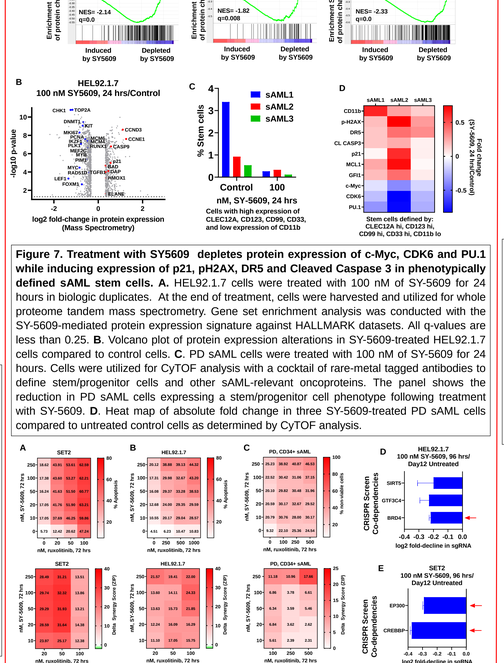

Figure 7. Treatment with SY5609 depletes protein expression of c-Myc, CDK6 and PU.1 while inducing expression of p21, pH2AX, DR5 and Cleaved Caspase 3 in phenotypically defined sAML stem cells. A. HEL92.1.7 cells were treated with 100 nM of SY-5609 for 24 hours in biologic duplicates. At the end of treatment, cells were harvested and utilized for whole proteome tandem mass spectrometry. Gene set enrichment analysis was conducted with the SY-5609-mediated protein expression signature against HALLMARK datasets. All q-values are less than 0.25. **B**. Volcano plot of protein expression alterations in SY-5609-treated HEL92.1.7 cells compared to control cells. **C**. PD sAML cells were treated with 100 nM of SY-5609 for 24 hours. Cells were utilized for CyTOF analysis with a cocktail of rare-metal tagged antibodies to define stem/progenitor cells and other sAML-relevant oncoproteins. The panel shows the reduction in PD sAML cells expressing a stem/progenitor cell phenotype following treatment with SY-5609. **D**. Heat map of absolute fold change in three SY-5609-treated PD sAML cells compared to untreated control cells as determined by CyTOF analysis.

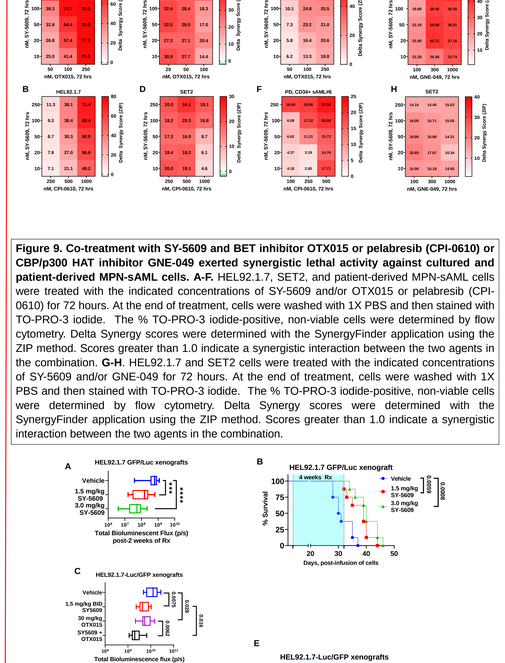

Figure 8. SY5609 exhibits synergistic lethal activity with ruxolitinib and a protein domain-specific CRISPR screen identified druggable co-dependencies and co-enrichments with SY-5609 treatment in HEL92.1.7 and SET2 cells. A-C. SET2, HEL92.1.7 and PD sAML cells were treated with the indicated concentrations of SY-5609 and/or ruxolitinib for 72 hours. The % TO-PRO-3 iodide positive, non-viable cells were determined by flow cytometry. Delta Synergy scores were determined with the SynergyFinder application using the ZIP method. Scores greater than 1.0 indicate a synergistic interaction between the two agents. **D-G**. HEL92 and SET2 Cas9-expressing cells were transduced with a library of guide RNAs against epigenetic modifier proteins. Eight days post transduction, cells were treated with 100 nM of SY-5609 for 4 days. Viable cells were harvested and genomic DNA was isolated and PCR amplified with guide RNA-specific primers. Amplicon-Seq (NGS) was performed to analyzed guide RNA abundance in the control and SY-5609-treated cells. Panels show the log2 fold-change in guide RNAs that were further depleted versus those that were co-enriched by treatment with SY-5609 ($p < 0.05$). Red arrows indicate druggable co-dependencies or co-enrichments with SY-5609 in the two cell lines.

Figure 9. Co-treatment with SY-5609 and BET inhibitor OTX015 or pelabresib (CPI-0610) or CBP/p300 HAT inhibitor GNE-049 exerted synergistic lethal activity against cultured and patient-derived MPN-sAML cells. A-F. HEL92.1.7, SET2, and patient-derived MPN-sAML cells were treated with the indicated concentrations of SY-5609 and/or OTX015 or pelabresib (CPI-0610) for 72 hours. At the end of treatment, cells were washed with 1X PBS and then stained with TO-PRO-3 iodide. The % TO-PRO-3 iodide-positive, non-viable cells were determined by flow cytometry. Delta Synergy scores were determined with the SynergyFinder application using the ZIP method. Scores greater than 1.0 indicate a synergistic interaction between the two agents in the combination. **G-H**. HEL92.1.7 and SET2 cells were treated with the indicated concentrations of SY-5609 and/or GNE-049 for 72 hours. At the end of treatment, cells were washed with 1X PBS and then stained with TO-PRO-3 iodide. The % TO-PRO-3 iodide-positive, non-viable cells were determined by flow cytometry. Delta Synergy scores were determined with the SynergyFinder application using the ZIP method. Scores greater than 1.0 indicate a synergistic interaction between the two agents in the combination.

Figure 10. Treatment with SY-5609-based combinations reduced leukemia burden and significantly improved survival of NSG mice bearing HEL92.1.7 xenografts. A. Total photon counts [flux] (determined by bioluminescent imaging) in NSG mice engrafted with luciferized HEL92.1.7 cells and treated for 2 weeks at the indicated doses. **B**. Kaplan-Meier survival plot of NSG mice and treated with the indicated doses of SY-5609 for 4 weeks. Significance was calculated by a Mantel-Cox log-rank test. **C**. Total photon counts [flux] (determined by bioluminescent imaging) in NSG mice engrafted with luciferized HEL92.1.7 cells and treated for 3 weeks with SY-5609 and/or OTX015 at the indicated doses. **D**. Representative bioluminescent images of mice from panel '**C**'. **E**. Kaplan-Meier survival plot of NSG mice engrafted with luciferized HEL92.1.7 cells and treated with SY-5609 and/or OTX015 at the indicated doses for 4 weeks. Significance between cohorts was determined by a Mantel-Cox log-rank test.

Conclusions

1. **Treatment with SY-5609 induced cell cycle G0/G1 arrest and loss of viability in cultured cells and PD CD34+ MPN-sAML cells while sparing normal CD34+ cells.**
2. **Knockout of CDK7 reduced c-Myc and PIM1 expression with concomitant induction of p21 and p27 expression and G0/G1 arrest in HEL92.1.7 cells. This led to reduced activity of CDK7 inhibitors SY-1365 and SY-5609.**
3. **RNA-Seq analysis of sAML cells treated with SY-5609 demonstrated significant reduction in the normalized enrichment scores for expression of gene-sets of MYC and E2F targets, as well as gene-sets for translation initiation and elongation.**
4. **Treatment with SY-5609 depleted leukemia relevant oncoproteins expressions in phenotypically defined sAML stem/progenitor cells**
5. **Compared to treatment with SY-5609, OTX015, or vehicle control, co-treatment with SY-5609 and OTX015 exerted superior in vivo anti-sAML efficacy and improved survival of mice bearing HEL92.1.7 xenografts.**
6. **These preclinical findings highlight the promise of SY-5609 treatment alone and in rational combinations in exerting significant anti-sAML efficacy against cellular models of sAML.**